

Development of Miscible Blends of Polyamide-6 and Manganese Sulfonated Polystyrene Using Specific Interactions

Xinya Lu and R. A. Weiss*

Polymer Science Program and Department of Chemical Engineering, University of Connecticut, Storrs, Connecticut 06269-3136

Received January 23, 1991; Revised Manuscript Received April 8, 1991

ABSTRACT: Interpolymer interactions involving manganese sulfonate and amide groups were used to develop miscible blends of polyamide-6 and a functionalized polystyrene containing 10.1 mol % manganese sulfonate groups. The polymers were miscible over the entire range of composition as evidenced by a single, composition-dependent T_g . The T_g 's for the blends exhibited positive deviation from a weight average of the two component polymer T_g 's. Interaction parameters, χ , were determined from melting point depression data. The χ 's were large and negative, indicating strong interactions between the component polymers. Infrared spectra confirmed that these specific interactions were hydrogen-bonding, ion-dipole, and complexation interactions involving the manganese sulfonate and amide groups.

Introduction

Polymer blending is a common and potentially versatile way to develop new materials with a desirable combination of properties. Because of unfavorable thermodynamics, however, it is difficult to obtain miscible compositions of two high molecular weight polymers. In the absence of specific intermolecular interactions, the free energy of mixing is usually positive for polymer blends due to a small combinatorial entropy of mixing and positive enthalpy of mixing. Over the past decade there has been considerable interest in enhancing the miscibility of polymer pairs either by adding a third component as a compatibilizing agent or by introducing specific functional groups into the polymers to promote exothermic interactions between them. Ionomers are particularly attractive materials for the latter approach.^{1,2}

Polyamide-6 (PA-6) is an important engineering thermoplastic. To improve its impact strength and moisture barrier properties, it is often blended with polyethylene (PE).³ It is difficult, however, to obtain good dispersion in such blends, and, in most practical examples, the PE was chemically modified or a third component was added to the blend to improve the compatibility. MacKnight et al.⁴ studied the blend of PA-6 and poly(ethylene-co-methacrylic acid) (PEMA) and observed that the size of the PEMA domains decreased with increasing methacrylic acid content. Research on a similar blend system by Fairley and Prud'homme⁵ indicated that PEMA interacted weakly with PA-6 and phase separation still occurred. Because sulfonic acid is a stronger acid than carboxylic acid, one might expect that a sulfonated ionomer will interact more strongly with PA-6 and provide better miscibility with PA-6. This is especially thought to be true when a transition-metal salt, such as manganese, that can complex with the amide groups is used. This paper describes the phase behavior of PA-6 and the manganese salt of lightly sulfonated polystyrene (MnSPS) blends. Specific attention is given to the associative interactions that occur in these blends.

Experimental Section

Sulfonated polystyrene (SPS) and its manganese salt (MnSPS) were prepared by the procedure described by Makowski et al.⁶ The starting polystyrene had a number-average molecular weight (M_n) of 100 000 and a weight-average molecular weight (M_w) of 280 000 as determined by gel permeation chromatography. The sulfonation level was 10.1 mol % as determined by titration of

the polymer in a toluene/methanol (10 vol % methanol) solution with sodium hydroxide in methanol. The salt was prepared by adding a 20% excess of manganese acetate in methanol to a solution of the SPS. The neutralized polymer was precipitated in a large excess of ethanol, filtered, washed several times with ethanol, and dried at 70 °C for 1 week under vacuum. PA-6 with a weight-average molecular weight of 24 000 was obtained from Polysciences Inc.

Blends of MnSPS and PA-6 with MnSPS concentration of 10, 20, 30, 40, 50, 60, and 80% by weight were prepared in *m*-cresol by adding a MnSPS solution dropwise into a stirred PA-6 solution. Films of the blends were cast from the solution at 140 °C and dried under vacuum at 90 °C for 2 weeks.

Thermal analysis of the blends was performed by using a Perkin-Elmer DSC-7 with a heating rate of 20 °C/min. The glass transition temperature (T_g) was defined as the midpoint of the change in the specific heat, and the melting point (T_m) was taken as the maximum of the melting endotherm. Isothermal crystallization from the melt was also examined by DSC. The samples were held at 240 °C for 5 min, quickly quenched to the crystallization temperature (T_c), and then kept at T_c for at least 30 min. After the isothermal crystallization was completed, the samples were cooled to 0 °C and heated to 250 °C at 20 °C/min to measure the melting temperature.

Infrared spectroscopy was used to assess the specific interactions that occurred between the two components of the blends. Spectra were measured with a Nicolet Model 60SX Fourier transform infrared (FTIR) spectrometer with a resolution of 1 cm⁻¹. The samples were cast on KBr plates from solution and dried under vacuum at 120 °C for at least 1 week.

Results and Discussion

Miscibility of the Blends. DSC thermograms of the component polymers and the blends are shown in Figure 1, and the values of T_g , T_m , and ΔH_m are summarized in Table I. Since the T_g 's of the component polymers were ca. 80 °C apart, the criterion of a single composition-dependent T_g could be used to assess miscibility of the blend. For all compositions, the blends exhibited only a single T_g intermediate between those of the pure constituents. The composition dependence of the T_g of the blends indicated that the amorphous phases of the two polymers were miscible. The blends with a MnSPS mass fraction $w_1 < 0.4$ exhibited a sharp glass transition, while the transition was considerably broadened for the blends with $w_1 > 0.6$. Broadening of the glass transition is generally an indication of local fluctuations in the blend composition.⁷ One possible explanation for this broadening is that the concentration of amide/manganese sulfonate interactions decreased with increasing MnSPS content, presumably

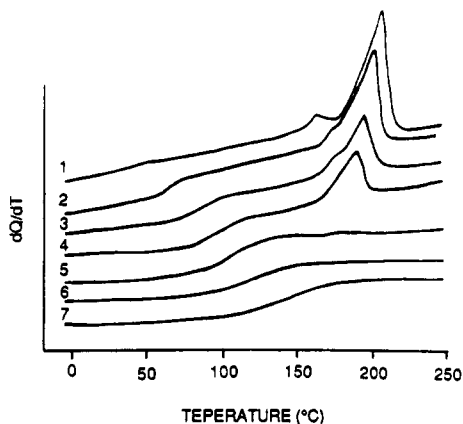


Figure 1. DSC thermograms of the PA-6/MnSPS blends: (1) 0% MnSPS; (2) 10 wt % MnSPS; (3) 20 wt % MnSPS; (4) 40 wt % MnSPS; (5) 60 wt % MnSPS; (6) 80 wt % MnSPS; (7) 100 wt % MnSPS.

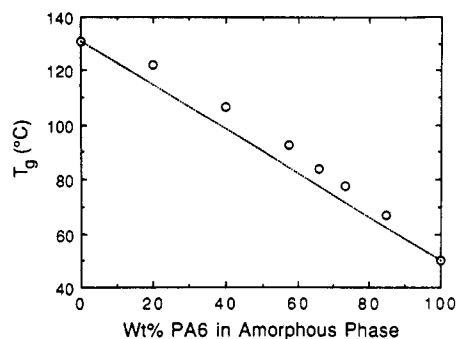


Figure 2. Composition dependence of T_g for the PA-6/MnSPS blends. Dotted line represents the weight average of the component T_g 's.

Table I
Thermal Transition Data for the Blends Measured by DSC

PA-6, wt %	T_g , °C	T_m , °C	ΔH_m , kJ/mol	PA-6, wt %	T_g , °C	T_m , °C	ΔH_m , kJ/mol
100	50.5	230.5	11.8	50	98.6		
90	66.0	228.8	7.8	40	106.7		
80	77.8	220.6	5.4	20	122.0		
70	84.2	211.3	2.9	0	131.5		
60	92.6	202.5	1.7				

due to increasing amounts of competing interpolymer association of the manganese sulfonate ion pairs.

In Figure 2, the glass transition temperatures are plotted as a function of the composition in the amorphous phase. The weight fraction of the amorphous phase of the PA-6 was determined by calculating the weight fraction of the crystalline phase. The latter was calculated from the ratio of the heat of melting of the PA-6 in the blend (ΔH_m) and that of 100% crystalline PA-6 (ΔH_u) = 18.1 kJ/mol.⁸ The experimentally determined T_g 's were higher than the value of the compositionally weighted linear average given by the dotted line in Figure 2. Positive deviation of the T_g of miscible blends is usually found in systems with strong interpolymer interactions, e.g., polymer-polymer complexes.⁹ In the case of PA-6/MnSPS blends, three types of interactions are possible: (1) hydrogen bonding between sulfonate and amide groups, (2) ion-dipole interaction between the ionic species and the polarized N-H bond, and (3) coordination of the transition-metal cation, Mn^{2+} , with the amide group.¹⁰ This will be discussed further later in this paper.

Melting Point of the Blends. The melting behavior of a blend with strong interactions is expected to be influenced by the miscible amorphous phase.⁷ A signif-

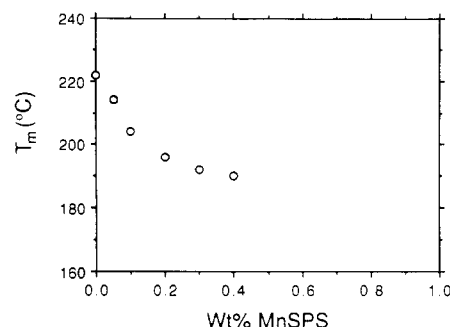


Figure 3. Variation of melting points of PA-6/MnSPS blends with composition.

Table II
Parameters for PA-6 and MnSPS

	PA-6	MnSPS		PA-6	MnSPS
V , cm ³ /g	0.917	0.892	ΔC_p , J/(g K)	0.37 ^b	0.33
ΔH_u , kJ/mol	18.1 ^a				

^a Heat of fusion of 100% crystalline PA-6.⁸ ^b ΔC_p of 100% amorphous PA-6; calculated as explained in the text.

icant melting point depression was observed for the PA-6/MnSPS blends, as shown by the T_m versus composition data in Figure 3. Crystallization was also influenced by the presence of MnSPS. No crystallinity was detected by DSC for the blends with $w_1 > 0.4$. The T_m depression of a crystallizable polymer in a miscible blend results either from a diluent effect or from changes in the crystalline morphology. The former effect can be treated by the equation of Nishi and Wang.¹¹

$$\frac{1}{T_m} - \frac{1}{T_m^0} = -\frac{\chi R V_{u2}}{V_{u1} \Delta H_{u2}} \Phi_1^2 \quad (1)$$

where the subscripts 1 and 2 refer to the noncrystallizable polymer and the crystallizable polymer, respectively. T_m and T_m^0 are the equilibrium melting points of the crystallizable component in the blend and in the neat polymer, respectively. The variables, Φ , V_u , and ΔH_u , are the normalized volume fraction, molar volume, and molar enthalpy of fusion of the component indicated. The values of ΔH_u , taken from the literature,⁸ V_u , calculated from the polymer density, and ΔC_p (the change in heat capacity associated with the glass transition), measured by DSC, are given in Table II. χ is the interaction parameter that measures the strength of the polymer-polymer interactions.

The morphological effect arises from the size of crystallites or the lamellar thickness L , as described by the following equation:¹²

$$T_{mL} = T_m(1 - 2\gamma_e/\Delta H_{u2}L) \quad (2)$$

where γ_e and L are respectively the interfacial energy and lamellar thickness. T_{mL} is the measured melting point corresponding to the lamellar thickness L . The morphological effect can be accounted for by the procedure of Hoffman and Weeks.¹² In this procedure, the lamellar thickness is controlled by varying the isothermal crystallization temperature. Data for different crystallization temperatures (T_c) are extrapolated to an infinitely large L , i.e., when the melting point coincides with the crystallization temperature, to determine T_m .

Figure 4 shows the application of the Hoffman-Weeks method for the MnSPS/PA-6 blends. The melting point, T_{mL} , increased linearly with the crystallization temperature (T_c) over a wide range of undercoolings, and it can

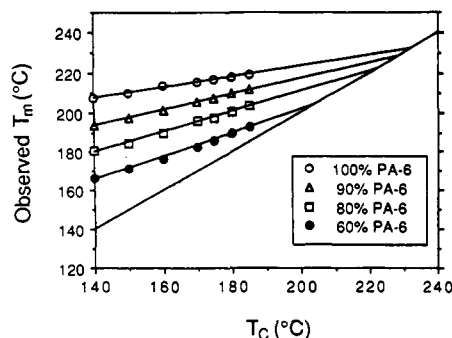


Figure 4. Hoffman-Weeks plots for PA-6/MnSPS blends. Equilibrium melting points were obtained by extrapolation of data to $T_c = T_m$ line.

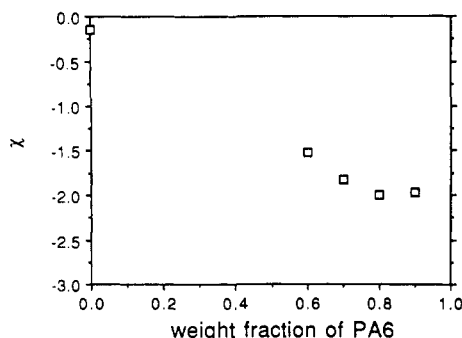


Figure 5. Interaction parameters for PA-6/MnSPS blends calculated from melting point depression data and eq 1.

be presented by the following equation:¹³

$$T_{mL} = [T_m(2\beta - 1) + T_c]/2\beta \quad (3)$$

where β is a morphological factor that represents the fold length in multiples of the primary and homogeneous nuclei. The values of the equilibrium melting points for the blends, obtained by the extrapolation of the lines in Figure 4 to $T_m = T_c$, are listed in Table I.

The compositional dependence of χ , as calculated from eq 1, is shown in Figure 5. The χ of the blend became less negative with increasing MnSPS content, which was consistent with the observed broadening of the glass transition at the higher MnSPS concentrations.

Predicted T_g of the Blends. Several theoretical equations, based on the assumption of random mixing at a segmental level, have been proposed to correlate the T_g and composition of miscible blends. Two of the more common ones are given in eqs 4 and 5.

Fox equation¹⁴

$$\frac{4}{T_g} = \frac{w_1}{T_{g1}} + \frac{w_2}{T_{g2}} \quad (4)$$

Couchman equation¹⁵

$$\ln T_g = \frac{w_1 \Delta C_{p1} \ln T_{g1} + w_2 \Delta C_{p2} \ln T_{g2}}{w_1 \Delta C_{p1} + w_2 \Delta C_{p2}} \quad (5)$$

where w_i is the weight fraction of polymer i . T_{gi} and ΔC_{pi} are the glass transition temperature and the heat capacity change at T_{gi} for polymer i , respectively. The experimental value of ΔC_p for MnSPS was 0.33 J/(g K). Direct measurement of ΔC_p for the 100% amorphous PA-6 is imprecise due to the difficulty in preparing a purely amorphous sample and the competing crystallization at the transition which obscures the true change in heat capacity in a DSC scan. Boyer¹⁶ proposed an empirical

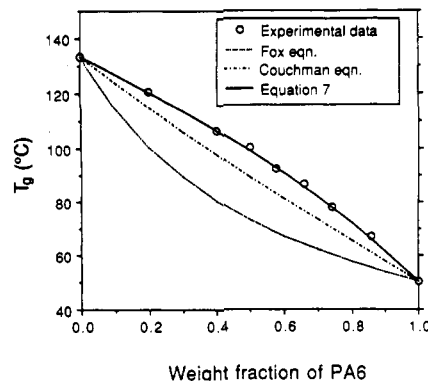


Figure 6. Comparison of experimental values and T_g 's predicted by eqs 4, 5, and 7.

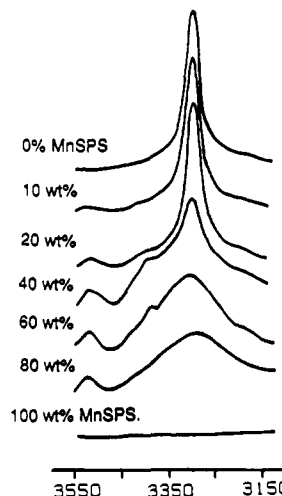


Figure 7. FTIR spectra in the N-H stretching region of the PA-6/MnSPS blends.

rule for amorphous polymers:

$$\Delta C_p T_g \text{ (J/g)} = 63 + 0.17 T_g \quad (6)$$

ΔC_p for PA-6 was estimated from eq 6 to be 0.37 J/(g K), and this value was used in eq 5 to calculate T_g of the blends. The predictions of the Fox and Couchman equations are plotted in Figure 6. The amorphous fraction of the PA-6 in the blends was determined by measuring the crystalline weight fraction as described previously. Both equations significantly underestimated the experimental values, which was probably due to the inability of these equations to take into account strongly exothermic interpolymer interactions. To account for the effect of specific interactions on T_g for a miscible blend, we have proposed the following equation:¹⁷

$$T_g = \frac{w_1 T_{g1} + k w_2 T_{g2}}{w_1 + k w_2} - \frac{\chi R (T_{g2} - T_{g1}) b w_1 w_2}{\Delta C_{p1} (w_1 + k w_2) (w_1 + b w_2)^2} \quad (7)$$

where $k = \Delta C_{p2} / \Delta C_{p1}$ and b is the ratio of the amorphous densities of polymer 2 and polymer 1. Equation 7 provides a relationship between the T_g and the thermodynamic interaction parameter χ . The χ 's for the PA-6/MnSPS blends were obtained from the melting point depression analysis, and eq 7 was used to predict the T_g of the blends. The blend T_g 's calculated from eq 7 are represented by the solid curve in Figure 6, which agrees well with the experimental data.

Interpolymer Interactions. Figure 7 shows the FTIR spectra of the PA-6/MnSPS blends in the 3150–3550-cm⁻¹ region, which corresponds to the N-H stretching vibration region. The frequency of the N-H stretching mode is

strongly dependent on the strength of the hydrogen-bonded N-H groups but essentially independent of the conformation.¹⁸⁻²⁰ For linear aliphatic polyamides, three N-H stretching bands occur at 3300, 3310, and 3447 cm^{-1} , which correspond to stretching vibrations of hydrogen-bonded N-H in the crystalline phase, hydrogen-bonded N-H in the amorphous phase, and "free" N-H groups, respectively.¹⁹ The spectrum of PA-6, as shown in Figure 7, is characterized by an absorption band centered at 3300 cm^{-1} . This band is believed to be a composite absorption consisting of hydrogen-bonded N-H stretching in the amorphous phase (at higher frequency) and that in the crystalline phase (at lower frequency).²⁰ When MnSPS was added to the PA-6, the band at 3300 cm^{-1} broadened, and the peak maximum for the completely amorphous blend (>60 wt % of MnSPS) was about 10 cm^{-1} lower than that of amorphous polyamide. This frequency shift could be due to either interpolymer interactions or dispersion effects, i.e., variation in refractive index. The latter possibility can be eliminated by comparison of the FTIR spectra of PA-6/MnSPS and PA-6/LiSPS blends (not shown). PA-6/LiSPS blends are also miscible at room temperature, but the interpolymer interactions in that system are weaker than in the PA-6/MnSPS system.²¹ Since LiSPS and MnSPS have nearly the same refractive index, any frequency shift of hydrogen-bonded N-H due to dispersion effects observed in the PA-6/MnSPS system should also occur in the PA-6/LiSPS system. This was not the case; for the amorphous blends of PA-6 and LiSPS (>80 wt % of LiSPS), the band for hydrogen-bonded N-H shifted to $\sim 3309 \text{ cm}^{-1}$. Thus, the shift to lower frequency of hydrogen-bonded N-H in the amorphous phase of the PA-6/MnSPS blend appears to have been due to stronger interactions, presumably hydrogen bonding, between the manganese sulfonate and the amide groups.

The broadening of the N-H stretching region with increasing MnSPS concentration probably indicates that there was a broad distribution of environments of the NH groups. Skrovanek et al.¹⁹ suggested that the position of the peak maximum for the hydrogen-bonded N-H stretching modes provides a measure of the average strength of the hydrogen bonds and the breadth of the band reflects the distribution of spatial orientation and separation of the interacting species.

Three effects tended to broaden the N-H stretching region of the FTIR spectra for the blends as the MnSPS concentration increased: (1) The volume fraction of the amorphous phase increased with increasing MnSPS content, and the distribution of hydrogen-bonded species in the amorphous phase is broader than in the crystalline phase; (2) the concentration of polyamide-polyamide hydrogen bonds decreased due to the competing interaction of the manganese sulfonate groups, which shifted the N-H stretching vibration to higher frequency; and (3) hydrogen bonding between the manganese sulfonate and amide groups shifted the N-H stretch to lower frequency.

Two absorption bands not observed in the neat PA-6 were found at 3410 and 3520 cm^{-1} in the FTIR spectra of the blends (Figure 7). Dunn et al.²² observed two similar bands, at 3400 and 3500 cm^{-1} , for PA-6 treated with nickel(II) chloride. They attributed these absorptions to non-hydrogen-bonded N-H stretching frequencies. On the basis of their conclusions, the two high-frequency bands observed in the MnSPS/PA-6 blends were assigned as follows. The band at 3410 cm^{-1} was notably lower than the free N-H stretching vibration that usually occurs at $\sim 3447 \text{ cm}^{-1}$.¹⁹ The shift to lower frequency suggests that the NH group coordinates with the Mn^{2+} transition-metal

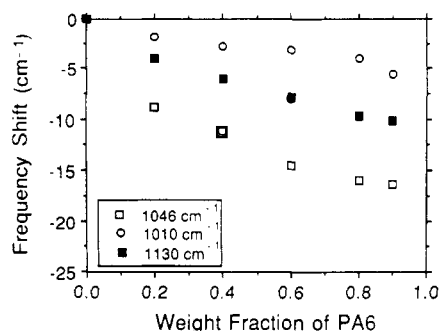


Figure 8. Frequency of the characteristic stretching bands of the SO_3Mn groups as a function of blend composition.

cation. Similarly, the band at 3520 cm^{-1} is believed to be due to delocalization of the lone-pair electrons on the nitrogen atom as a result of interaction with the Mn^{2+} cation.

Confirmation that the sulfonate group was involved in the interactions was obtained from changes in the absorption bands characteristic of the stretching vibration of the manganese sulfonate group. Interactions involving the manganese sulfonate groups should shift these vibrations to lower frequencies.¹⁰ Figure 8 shows the frequencies of three absorption bands due to manganese sulfonate as a function of the blend composition. As the PA-6 content increased, the bands at 1130, 1047, and 1010 cm^{-1} shifted to 1119, 1029, and 1006 cm^{-1} , respectively. These shifts to lower frequencies are the consequence of specific interpolymer interactions involving the manganese sulfonate. Similar frequency shifts were observed by Fitzgerald and Weiss²³ for NaSPS swelled with dimethylformamide. For example, the symmetric stretching vibration of the sulfonate group moved from 1048 to 1034 cm^{-1} , due to the interactions between the sodium sulfonate and amide groups.

Conclusion

Hydrogen-bonding, ion-dipole, and transition-metal complexation between manganese sulfonate and amide groups enhanced the miscibility of polyamide-6 and lightly sulfonated polystyrene. Thermal analysis indicated that the two polymers were miscible over the entire range of composition. The T_g 's of the blends exhibited a large positive deviation from the weight average of the individual component T_g 's. This was similar to the behavior of interpolymer complexes and suggested that the interactions between the two polymers were strong. The interaction parameter, χ , of the blend was calculated from the melting point depression data and had a large negative value. This result also indicates that strong interactions occurred between the two polymers. FTIR provided further evidence of specific interpolymer interactions involving the manganese sulfonate and amide groups.

Acknowledgment. We are grateful for the support of this research by the Polymers Program of the National Science Foundation, Division of Materials Research, Grant DMR 88-05981.

References and Notes

- (1) Smith, P.; Hara, M.; Eisenberg, A. In *Current Topics in Polymer Science, II*; Ottenbrite, R. M., Utracki, L. A., Inoue, S., Eds.; Hanser: New York, 1987; p 255.
- (2) Weiss, R. A.; Beretta, C.; Sasongko, S.; Garton, A. *J. Appl. Polym. Sci.* 1990, 41, 91.
- (3) Kamal, M. R.; Jinnah, I. A.; Utracki, L. A. *Polym. Eng. Sci.* 1984, 24, 1337.

- (4) MacKnight, W. J.; Lenz, R. W.; Musto, P. V.; Somani, R. J. *Polym. Eng. Sci.* **1985**, *25*, 1124.
- (5) Fairley, G.; Prud'homme, R. E. *Polym. Eng. Sci.* **1987**, *27*, 1495.
- (6) Makowski, H. S.; Lundberg, R. D.; Singhal, G. H. U.S. Patent 3,870,841, 1975.
- (7) Olabisi, O.; Robeson, L. M.; Shaw, M. T. *Polymer-Polymer Miscibility*; Academic Press: New York, 1979.
- (8) Rybníkar, F. *Collect. Czech. Chem. Commun.* **1959**, *24*, 2861.
- (9) Rodriguez-Parada, J. M.; Percec, V. *Macromolecules* **1986**, *19*, 55.
- (10) Zundel, G. *Hydration and Intermolecular Interaction*; Academic Press: New York, 1969; Chapter IV.
- (11) Nishi, T.; Wang, T. T. *Macromolecules* **1975**, *8*, 909.
- (12) Hoffman, J. D.; Weeks, J. J. *J. Res. Natl. Bur. Stand.* **1962**, *66A*, 13.
- (13) Hoffman, J. D. *Polymer* **1982**, *23*, 656.
- (14) Fox, T. G. *Bull. Am. Phys. Soc.* **1956**, *1*, 123.
- (15) Couchman, P. R. *Macromolecules* **1978**, *11*, 1156.
- (16) Boyer, R. F. *J. Macromol. Sci., Phys.* **1973**, *B7*, 487.
- (17) Lu, X.; Weiss, R. A. *Polym. Prepr. (Am. Chem. Soc., Div. Polym. Chem.)* **1991**, *32* (1).
- (18) Trifan, D. S.; Terenzi, J. F. *J. Polym. Sci.* **1958**, *28*, 443.
- (19) Skrovanek, D. J.; Painter, P. C.; Coleman, M. M. *Macromolecules* **1986**, *19*, 699.
- (20) Skrovanek, D. J.; Stephen, E. H.; Painter, P. C.; Coleman, M. M. *Macromolecules* **1985**, *18*, 1676.
- (21) Lu, X.; Weiss, R. A. Proceedings of the Fall Meeting of the Materials Research Society, 1990.
- (22) Dunn, P.; Sanson, G. F. *J. Appl. Polym. Sci.* **1969**, *13*, 1657.
- (23) Fitzgerald, J. J.; Weiss, R. A. In *Coulombic Interactions in Macromolecular Systems*; Eisenberg, A., Bailey, F. E., Eds.; ACS Symposium Series 302; American Chemical Society: Washington, DC, 1986; p 35.